Journal of Sound and Vibration (1996) **193**(5), 1023–1035

INTERNAL RESONANCE OF AN L-SHAPED BEAM WITH A LIMIT STOP: PART I, FREE VIBRATION

D. Pun, S. L. Lau and Y. B. Liu†

Department of Civil and Structural Engineering, Hong Kong Polytechnic University, Hung Hom, Hong Kong

(*Received* 23 *August* 1994, *and in final form* 20 *October* 1995)

Real-life structures often possess piecewise stiffness because of clearances or interference between subassemblies. Such an aspect can alter a system's fundamental free vibration response and leads to complex mode interaction. The free vibration behaviour of an L-shaped beam with a limit stop is analyzed by using the frequency response function and the incremental harmonic balance method. The presence of multiple internal resonances, which involve interactions among the first five modes and are extremely complex, have been discovered by including higher harmonics in the analysis. The results show that mode interaction may occur if the higher harmonics of a vibration mode are close to the natural frequency of a higher mode. The conditions for the existence of internal resonance are explored, and it is shown that a prerequisite is the presence of bifurcation points in the form of intersecting backbone curves. A method to compute such intersections by using only one harmonic in the free vibration solution is proposed.

1. INTRODUCTION

A piecewise linear stiffness characteristic is inadvertently present in many structural systems. Quite often this is caused by a small gap or space between components or assemblies. For example, clearances between structural parts in mechanical equipment are usually incorporated for the normal operation of the equipment. Under some circumstances such a space is taken up by excessive movement or deflection due to extreme loads and the resulting interference between subassemblies may induce piecewise linear response. Another common cause of this behaviour is the bottoming out of a spring when its travel has been completely taken up under abnormal conditions. In structural applications gaps are sometimes introduced to suit the intended manner of support under different load situations, for instance, in the use of snubber supports against earthquake loads. There are also cases in which the chosen means of support leads to inevitable construction clearances, such as the use of frame supports in lieu of welded attachments for piping systems. The existence of piecewise linear stiffness means that the vibration of the system under dynamic loading is basically non-linear, as demonstrated by Wong et al. [1]. Lau and Zhang [2] have used the incremental harmonic balance (IHB) method to compute the subharmonic and superharmonic responses of a single-degree-of-freedom spring under periodic loading.

Murakami and Sato [3] analyzed and tested the forced vibration behaviour of an L-shaped beam with a limit stop. They used a describing function approach which is

† Permanent Address: Institute of Mechanics, Chinese Academy of Science, Beijing 100080, People's Republic of China.

0022–460X/96/251023 + 13 $18.00/0

basically a one harmonic approximation of the response, and found that the usual hardening behaviour is present once the maximum deflection of the beam exceeds the clearance of the stop. The free vibration behaviour of the beam is analyzed here through the use of the IHB method, because this approach allows the solution to be expressed as a Fourier series. The study of free vibration is of significance, as such a response encompasses the intrinsic dynamic characteristics of the system and therefore is fundamental to the understanding of the problem. The formulation of the equation of motion is first carried out and the solution process by the IHB procedure is outlined. The structure is then shown to possess intricate internal resonances which can only be unearthed by including higher harmonics in the assumed solution series. The complex characteristics of modal interaction are then explained, and the conditions for the existence of internal resonance in piecewise linear systems are examined in some detail.

2. FREE VIBRATION FORMULATION

The formulation for the free vibration analysis of a linear structure coupled to a grounded piecewise linear spring is presented below. The spring is represented by its internal force in the equation of motion, which is:

$$[\mathbf{M}]\{\mathrm{d}^2\mathbf{z}/\mathrm{d}t^2\} + [\mathbf{K}]\{\mathbf{z}\} + \{\mathbf{f}\} = \{\mathbf{0}\}, \tag{1}$$

where [**M**], and [**K**] are the mass and stiffness matrices of the L beam, and $\{\mathrm{d}^2\mathbf{z}/\mathrm{d}t^2\}$, $\{\mathbf{z}\}$ are the normalized nodal acceleration and displacement vectors, respectively, as these are expressed as ratios to the stop clearance z_c. $\{\mathbf{f}\}$ is the force vector containing the internal force f of the spring at the degree of freedom (d.o.f.) 7 where the spring is connected to the structure:

$$\{\mathbf{f}\} = [0, 0, 0, 0, 0, 0, f, 0, 0, 0, 0]^{\mathrm{T}}. \tag{2}$$

Here 11 d.o.f.s are used to model the structure. The constitutive relationship of the piecewise linear stiffness element is

$$f(z) = \rho A l \omega_1^2 z_c \begin{cases} k_1 + k_2(z-1), & z > 1 \\ k_1 z, & |z| \le 1 \\ -k_1 + k_2(z+1), & z < -1 \end{cases}, \tag{3}$$

with

$$k_1 = K_1/\rho A l \omega_1^2 \qquad k_2 = K_2/\rho A l \omega_1^2 \qquad z = \Delta/z_c.$$

Here Δ is the deflection at node 7, K_1 is the stiffness for Δ less than or equal to z_c and K_2 is the stiffness for larger deflection. For ease of discussion the dimensionless quantities z, k_1, k_2 corresponding to the physical quantities Δ, K_1, K_2, respectively, are introduced. These are normalized with respect to the following beam parameters: ρ the mass density, A the cross-section area, l the total L-span length, and ω_1 the first linear natural frequency.

Upon introducing the non-dimensional time $\tau = \omega t$, equation (1) can be rewritten as

$$\omega^2[\mathbf{M}]\{\ddot{\mathbf{z}}\} + [\mathbf{K}]\{\mathbf{z}\} + \{\mathbf{f}\} = \{\mathbf{0}\}, \tag{4}$$

where $\cdot$ denotes differentiation with respect to τ.

3. IHB METHOD

For free vibration analysis, the displacement $\{\mathbf{z}\}$ can be expressed as a cosine series and the acceleration $\{\ddot{\mathbf{z}}\}$ can be obtained by differentiation:

$$\{\mathbf{z}\} = \left(\frac{\mathbf{a}_0}{2}\right) + \sum_{n=1}^{NH} \{\mathbf{a}_n\} \cos n\tau, \qquad \{\ddot{\mathbf{z}}\} = \sum_{n=1}^{NH} -n^2\{\mathbf{a}_n\} \cos n\tau \tag{5, 6}$$

Here $\{\mathbf{a}_0/2\}$, $\{\mathbf{a}_n\}$ are the series coefficients of the displacement, and NH is the number of harmonic terms whose appropriate value depends on the desired accuracy. Likewise, the non-linear member force f can be expanded as

$$f = (u_0/2) + \sum_{n=1}^{NH} u_n \cos n\tau, \tag{7}$$

where the coefficients of the non-linear spring force at d.o.f. 7, $u_0/2$ and u_n are formally given by

$$u_0 = \frac{1}{2\pi}\int_0^{2\pi} f(z)\, \mathrm{d}\tau, \qquad u_n = \frac{1}{n}\int_0^{2\pi} f(z) \cos n\tau\, \mathrm{d}t, \qquad n = 1, 2, \ldots, NH, \tag{8}$$

The evaluations of the integral in equation (8) depend on whether or not $|z|$ is greater than 1 and the explicit formulae have been worked out by Lau and Zhang [2]. With equations (2) and (7), the vector $\{\mathbf{f}\}$ can be expressed as

$$\{\mathbf{f}\} = \{\mathbf{s}_0/2\} + \sum_{n=1}^{NH} \{\mathbf{s}_n\} \cos n\tau, \tag{9}$$

where

$$\{\mathbf{s}_0/2\} = [0, 0, 0, 0, 0, 0, u_0/2, 0, 0, 0, 0]^{\mathrm{T}}, \qquad \{\mathbf{s}_n\} = [0, 0, 0, 0, 0, 0, u_n, 0, 0, 0, 0]^{\mathrm{T}}, \tag{10}$$

$\{\mathbf{s}_0/2\}$ and $\{\mathbf{s}_n\}$ being the harmonic components of the non-linear force vector. Substituting equations (5), (6) and (9) into equation (4), and applying the Galerkin procedure, one can obtain the following non-linear equations:

$$[\mathbf{K}]\{\mathbf{a}_0/2\} + \{\mathbf{s}_0/2\} = \{\mathbf{0}\}, \qquad [\mathbf{K}_D(n\omega)]\{\mathbf{a}_n\} + \{\mathbf{s}_n\} = \{\mathbf{0}\}, \qquad n = 1, 2, \ldots, NH. \tag{11}$$

Here $[\mathbf{K}_D(n\omega)]$ is the dynamic stiffness matrix for the harmonic term n:

$$[\mathbf{K}_D(n\omega)] = [\mathbf{K}] - n^2\omega^2[\mathbf{M}], \qquad n = 1, 2, \ldots, NH. \tag{12}$$

The dynamic flexibility matrix $[\mathbf{H}(n\omega)]$ (receptance or transfer function matrix) for the harmonic term n is the inverse of $[\mathbf{K}_D(n\omega)]$; i.e.,

$$[\mathbf{H}(n\omega)] = [\mathbf{K}_D(n\omega)]^{-1}, \qquad n = 1, 2, \ldots, NH. \tag{13}$$

Also, it can be seen clearly that

$$[\mathbf{H}(0)] = [\mathbf{K}]^{-1}, \tag{14}$$

The explicit formulae for $[\mathbf{H}(n\omega)]$ can be obtained by using the solution of the eigenvalue problem $[\mathbf{K} - \omega^2\mathbf{M}]\mathbf{\Phi} = \{\mathbf{0}\}$, where $\mathbf{\Phi}$ are the eigenvectors of the L beam.

Premultiplying equation (11) by the dynamic flexibility matrix gives

$$\{\mathbf{a}_0/2\} + [\mathbf{H}(0)]\{\mathbf{s}_0/2\} = \{\mathbf{0}\}, \qquad \{\mathbf{a}_n\} + [\mathbf{H}(n\omega)]\{\mathbf{s}_n\} = \{\mathbf{0}\}, \qquad n = 1, 2, \ldots, NH, \tag{15}$$

Upon substituting equation (10) into equation (15), $a_{k0}/2$ and a_{kn}, the displacement harmonics 0 and n for the d.o.f. k can be written as

$$(a_{k0}/2) + H_{k7}(0)(u_0/2) = 0, \qquad k = 1, 2, \ldots, 11,$$

and

$$a_{kn} + H_{k7}(n\omega)u_n = 0, \qquad n = 1, 2, \ldots, NH. \tag{16}$$

Equations (16) are the harmonic balance equations for all the degrees of freedom. Since u_0 and u_n ($n = 1, 2, \ldots, NH$) are functions only of the displacements a_{70} and a_{7n}, one can conclude that only the equations relating to a_{70} and a_{7n} need to be solved. The other coefficients can be found by back substitution. Upon simplifying notations by using a_n to denote a_{7n}, introducing the vectors of length $(NH + 1)$,

$$\{\mathbf{c}\} = [a_0/2, a_1, \ldots, a_{NH}]^{\mathrm{T}}, \qquad \{\mathbf{r}\} = [u_0/2, u_1, \ldots, u_{NH}]^{\mathrm{T}}, \tag{17, 18}$$

and a $(NH + 1) \times (NH + 1)$ matrix

$$[\mathbf{Y}] = \begin{bmatrix} H_{77}(0) & 0 & \ldots & 0 \\ 0 & H_{77}(\omega) & \ldots & 0 \\ \vdots & \vdots & \ddots & \vdots \\ 0 & 0 & \ldots & H_{77}(NH\omega) \end{bmatrix}, \tag{19}$$

equation (16) can be expressed in matrix form as

$$\{\mathbf{c}\} + [\mathbf{Y}]\{\mathbf{r}\} = \{\mathbf{0}\}, \tag{20}$$

with the residual vector $\{\boldsymbol{\varepsilon}\}$ defined as

$$\{\boldsymbol{\varepsilon}\} = \{\mathbf{c}\} + [\mathbf{Y}]\{\mathbf{r}\}, \tag{21}$$

for equilibrium one has

$$\{\boldsymbol{\varepsilon}\} = \{\mathbf{0}\}. \tag{22}$$

Equation (22) is a set of non-linear algebraic equations. The Newton–raphson procedure can be used to solve for the unknowns which are the harmonic coefficients of the displacement at the elbow of the L beam. In this process the new values $\{\mathbf{c}\}$, ω are obtained by adding the increments $\{\Delta\mathbf{c}\}$, $\Delta\omega$ to the current values $\{\mathbf{c}_0\}$, ω_0. Hence

$$\{\mathbf{c}\} = \{\mathbf{c}_0\} + \{\Delta\mathbf{c}\}, \qquad \omega = \omega_0 + \Delta\omega. \tag{23}$$

Expanding equation (22) as a one-term Taylor series and noting that $\{\boldsymbol{\epsilon}\}$ vanishes for a correct solution, one finds

$$\{\boldsymbol{\varepsilon}_0\} + \partial\{\boldsymbol{\varepsilon}\}/\partial\{\mathbf{c}\}|_0\{\Delta\mathbf{c}\} + \partial\{\boldsymbol{\varepsilon}\}/\partial\omega|_0\,\Delta\omega = \{\mathbf{0}\}, \tag{24}$$

where

$$\partial\{\boldsymbol{\varepsilon}\}/\partial\{\mathbf{c}\} = -[\mathbf{I}] - [\mathbf{Y}]\,\partial\{\mathbf{r}\}/\partial\{\mathbf{c}\}, \qquad \partial\{\boldsymbol{\varepsilon}\}/\partial\omega = (\partial[\mathbf{Y}]/\partial\omega)\{\mathbf{r}\} + [\mathbf{Y}]\,\partial\{\mathbf{r}\}/\partial\omega, \tag{25, 26}$$

[**I**] being the identity matrix. Let

$$\{\mathbf{h}\} = [\tfrac{1}{2}, \cos\tau, \ldots, \cos NH\tau]^{\mathrm{T}}. \tag{27}$$

Then

$$\{\mathbf{r}\} = \frac{1}{\pi}\int_0^{2\pi} \{\mathbf{h}\} f(\mathbf{z})\, \mathrm{d}\tau, \qquad \mathbf{z} = \{\mathbf{h}\}^{\mathrm{T}}\{\mathbf{c}\}. \tag{28, 29}$$

The derivatives with respect to ω and $\{\mathbf{c}\}$ are

$$\frac{\partial\{\mathbf{r}\}}{\partial\omega} = \frac{1}{\pi}\int_0^{2\pi} \{\mathbf{h}\} \frac{\partial f(\mathbf{z})}{\partial\omega}\, \mathrm{d}\tau = \{\mathbf{0}\}, \tag{30}$$

$$\frac{\partial\{\mathbf{r}\}}{\partial\{\mathbf{c}\}} = \frac{1}{\pi}\int_0^{2\pi} \{\mathbf{h}\} \frac{\partial f(\mathbf{z})}{\partial\mathbf{z}} \frac{\partial\mathbf{z}}{\partial\{\mathbf{c}\}}\, \mathrm{d}\tau = \frac{1}{\pi}\int_0^{2\pi} \{\mathbf{h}\} \frac{\partial f(\mathbf{z})}{\partial\mathbf{z}} \{\mathbf{h}\}^{\mathrm{T}}\, \mathrm{d}\tau, \tag{31}$$

and $\partial[\mathbf{Y}]/\partial\omega$ can be obtained from equations (12)–(14). Then the solution of equation (24) can be found by the following iterative steps:

$$-\partial\{\boldsymbol{\varepsilon}\}/\partial\{\mathbf{c}\}|_i \{\Delta\mathbf{c}_{i+1}\} = \{\boldsymbol{\varepsilon}_0\}|_i + \partial\{\boldsymbol{\varepsilon}\}/\partial\omega|_i \Delta\omega_{i+1}, \qquad \{\mathbf{c}\}_{i+1} = \{\mathbf{c}\}_i + \{\Delta\mathbf{c}\}_{i+1},$$
$$\omega_{i+1} = \omega_i + \Delta\omega_{i+1}. \tag{32, 33a, b}$$

It should be noted that one element of $\{\mathbf{c}_i\}$ or ω should be fixed in performing the above iterations.

4. RESULTS AND DISCUSSION

4.1. Mode Interaction

The L beam shown in Figure 1 comprising spans l_1 and l_2 lies in the XY plane with d.o.f. displacement z, rotation about the x-axis θ_x, and rotation about the y-axis θ_y. The beam's ends are completely fixed and there is a limit stop at the junction of the two spans l_1 and l_2 which inhibits movement once the deflection Δ there exceeds the clearance z_c. The stiffness of the stop is taken to be linear so the beam-stop structure exhibits piecewise linear stiffness characteristics. The beam properties are as follows: Young's modulus $E = 216\,000$ MPa, Poisson's ratio $\mu = 0{\cdot}3$, density $\rho = 8880$ kg/m^3, area $A = 50$ mm^2, moment of inertia $I = 104{\cdot}167$ mm^4, torsion inertia $J = 416{\cdot}607$ mm^4, gap $z_c = 1$ mm,

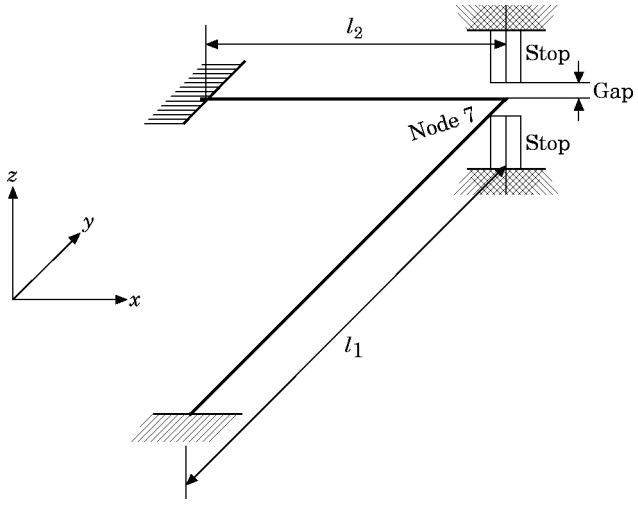

Figure 1. L beam with a limit stop.

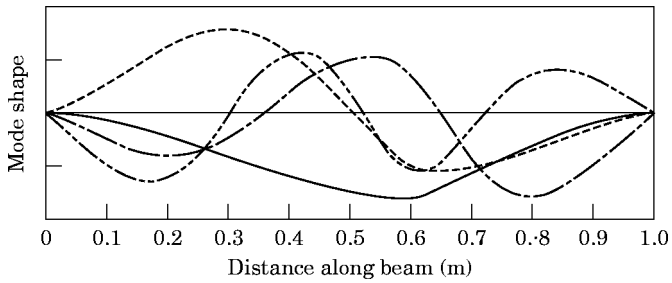

Figure 2. Linear mode shapes of L beam, ——, 1st mode; - - - - - - , 2nd mode; – · – · –, 3rd mode; – · · – · · –, 4th mode.

spans $l_1 = 0{\cdot}6$ m and $l_2 = 0{\cdot}4$ m. The beam is modelled by using 11 finite elements and its first four linear vibration mode shapes are shown in Figure 2. The first five actual natural (ω_i) and normalized ($\Omega_i = \omega_i/\omega_1$) frequencies are listed in Table 1.

With $k_1 = 0.0025$ and $k_2 = 5$ to model a nearly rigid stop, 10 modes to calculate the dynamic stiffness matrix, and five odd harmonic terms for the IHB solution, the free vibration response of the structure has been obtained and results are shown in Figure 3. The diagram is a plot of the normalized physical amplitudes of the ith harmonic z_i at node 7 (L junction) against the normalized frequency $\Omega = \omega/\omega_1$, where ω is the excitation frequency. Note that z_n is actually vibrating at a frequency of $n\omega$; the shift of the abscissa by $1/n$ is logical because all the harmonics are vibrating simultaneously. Clearly it can be seen that the response is complicated with internal resonance occurring at Ω of about 1·02, 1·23 and 1·27 (points B, C, D respectively) which a one-harmonic solution could not capture.

Figure 4 is a clearer view of the region around $\Omega = 1$ in which z_5, z_7 and z_9 are not shown as these values are negligible in this area. For z_1 less than 1 the structure behaves linearly and the higher harmonics are zero. For z_1 equal to 1 or larger the hard spring is engaged and z_3 becomes finite but small. As Ω increases from 1 both z_1 and z_3 gradually increases with the former being dominant and the two having opposite phases; for instance, at $\Omega = 1{\cdot}022$, $z_1 = 1{\cdot}163$ and $z_3 \approx -0{\cdot}2$. The non-linear deflected shapes for the first and third harmonics closely resemble the first and second linear modes because Ω and 3Ω are close to the first and second normalized linear frequencies, respectively. The resultant displacement profile is similar to that of the first linear mode as z_i is significantly larger than z_3 in this frequency range. The vibration behaviour is more complicated in the range of Ω from 1·023 to 1·027. As Ω moves past the first natural frequency ($\Omega = 1$), z_1 and z_3 would have followed smooth extensions from points A and A′, respectively, in the absence of internal resonance. However, as 3Ω is close to Ω_2 the system's propensity for vibrating in the second mode is sufficient to cause the z_1 and z_3 curves to reverse to points

TABLE 1

Natural frequencies of L beam

Mode i	ω_i(rad/s)	Ω_i
1	138·1	1·00
2	423·9	3·07
3	727·5	6·16
4	1223·0	8·92
5	2167·0	15·68

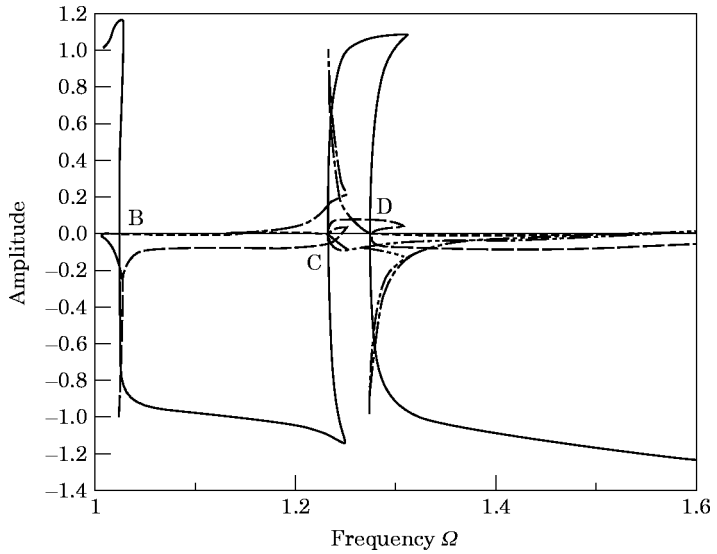

Figure 3. Backbone curves for $\Omega = 1{\cdot}00$–$1{\cdot}60$, —— z_1; - - - - - - z_3; – · – · – z_5; – · · – · · – z_7; · · · · · · z_9.

B and B′ (see Figure 4), respectively, at the interaction frequency $\Omega \approx 1$. The structure is now vibrating in the second mode as $z_1 = 0$ and $z_3 = 1$. Furthermore, because of the pattern traced out by these components, the displacement profile is no longer unique and up to three different non-linear modes are possible for some Ω. That the point B′ on the z_3 curve is precisely at $\Omega_2/3$ is inherent for piecewise linear systems, in contrast with continuously non-linear ones for which this point would be offset from its corresponding linear frequency. The seemingly complicated trajectories can be seen in a much more straightforward light if it is recognized that points B are pivotal in this response.

As Ω further increases past $1{\cdot}023$ and 3Ω begins to move away from Ω_2, z_1 becomes progressively larger and z_3 correspondingly smaller, with the total magnitude $z_1 + z_3$ always

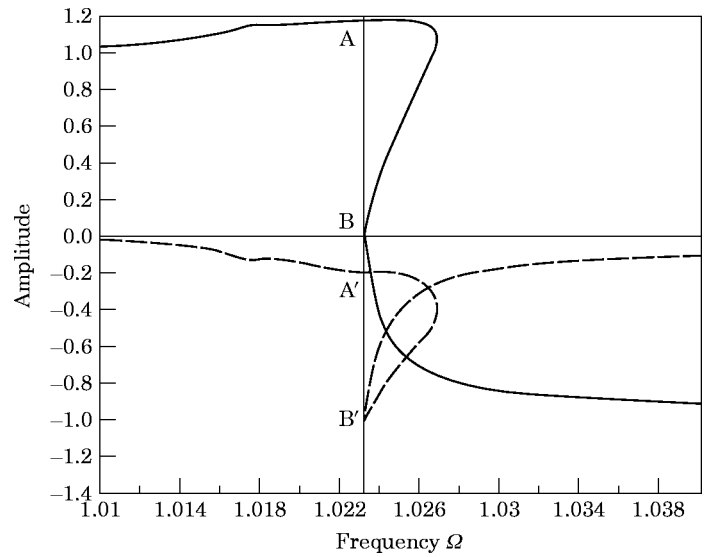

Figure 4. Amplitudes z_1 and z_3 for $\Omega = 1{\cdot}01$–$1{\cdot}04$. —— z_1, - - - - - - z_3.

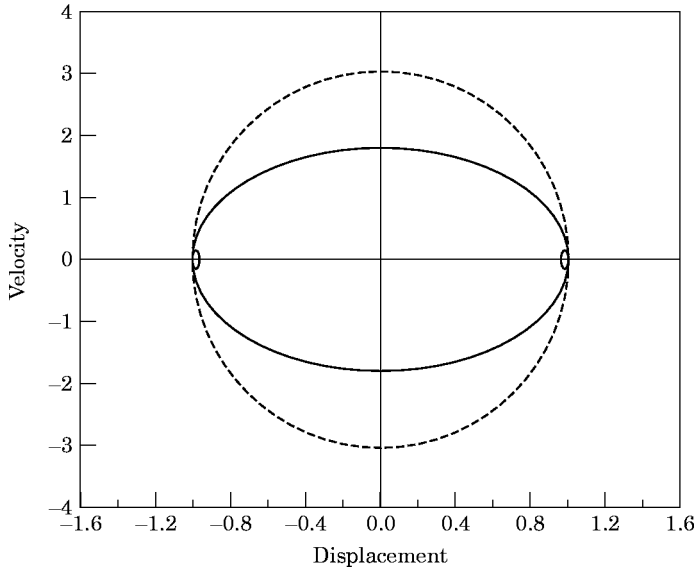

Figure 5. Phase diagrams for points A and B. —— A; - - - - - - *B*.

equal to approximately -1, signifying that the stop is engaged throughout this frequency range. The system's phase diagrams at points A and B are shown in Figure 5 and it can be seen that at point A the stop is impacted four times per period $T = 2\pi/\Omega$ and at point B the hit frequency is two times per period $T = 2\pi/3\Omega$.

At $\Omega = 1{\cdot}232$ a second internal resonance takes place; this time the interaction is between the first and fifth harmonic. However, the solution curves in this region are complicated by the existence of another resonance nearby at $\Omega = 1{\cdot}274$, where the first and the seventh harmonics participate in an exchange of energy. From Figure 6 it can be seen that as Ω approaches 1·232, z_1 continues its typical hardening trend of increasing at a moderate pace,

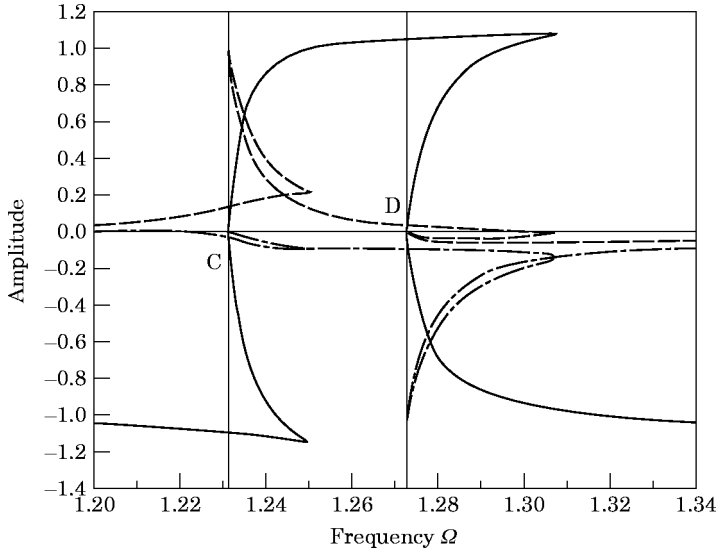

Figure 6. Amplitudes z_1, z_5, z_7 for $\Omega = 1{\cdot}20$–$1{\cdot}34$. —— z_1; - - - - - - z_5; – · – · – z_7.

and both z_5 and z_7 begin to increase. The amplitudes of z_3 and z_9 are negligible and are not shown. z_3 decreases in this region because Ω is moving away from Ω_2 and z_5 increases because Ω is close to $\Omega_3/5$. The increase in z_7 is small but noticeable and is attributed to Ω's proximity to $\Omega_4/7$. The displacement profiles for z_1, z_3, z_5 and z_7 are similar to those of the first, second, third and fourth linear modes, respectively. As Ω continues to increase beyond 1·232, z_1 reverses direction and drops to 0 at point C where Ω is equal to 1·232, and this pattern is also repeated by z_3 and z_7. z_5, on the contrary, ascends steeply to a magnitude of 1 as the beam is now vibrating at the third normalized linear frequency. It is noticed that in the course of its pullback z_1 crosses the Ω axis and changes phases at $\Omega = 1{\cdot}232$, unlike z_5 and z_7 which form completely reversed loops during this interaction. Finally there is a third internal resonance at $\Omega = 1{\cdot}274$, a frequency equal to 1/7 of the fourth normalized linear frequency. Accordingly the interaction is then between the first and seventh harmonic, and the beam vibrates principally in its fourth natural mode at point D of Figure 6.

The cases illustrated so far are concerned principally with the interaction between the first linear mode and other higher modes. However, there are also internal resonances involving the second mode and other higher modes, for instance as $\Omega_5 = 5{\cdot}111\Omega_2$, the fifth harmonic tends to increase substantially in amplitude when $\Omega = 3{\cdot}136$, because then $5\Omega = 15{\cdot}680$. In this particular case the interaction is between the second and the fifth linear mode, as Ω is close to Ω_2 and 5Ω equals Ω_5, the results are shown in Figure 7.

4.2. The existence of internal resonance

That a system's linear eigenvalues being integer multiples of each other is not sufficient to give rise to internal resonance is well known (see, for instance, reference [4]). It is the presence of bifurcation points in the form of intersections of the backbone curves for the different modes that permit modal interaction. For systems with piecewise linear stiffness such curves can readily be computed by using the present algorithm.

Consider a linear structure idealized as a two-mode model with normalized frequencies Ω_1 and Ω_2 for which the ratio Ω_2/Ω_1 is close to an integer n. The structure is coupled at

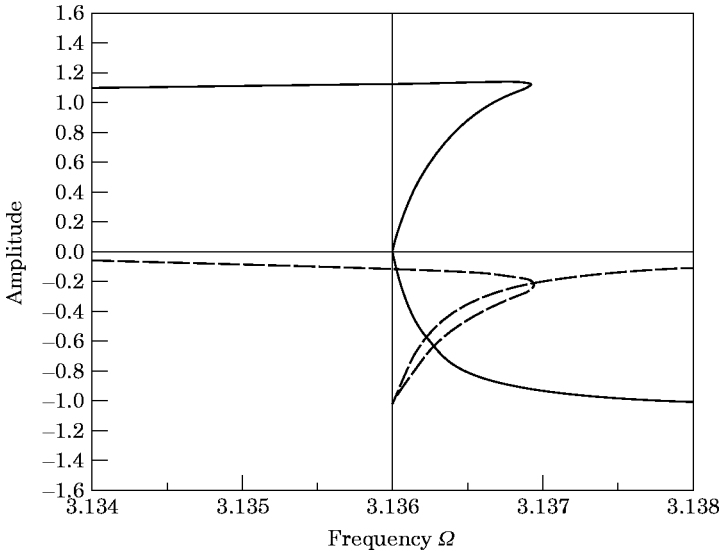

Figure 7. Amplitudes z_1, z_5 for $\Omega = 3{\cdot}134$–$3{\cdot}138$. —— z_1; - - - - - - z_5.

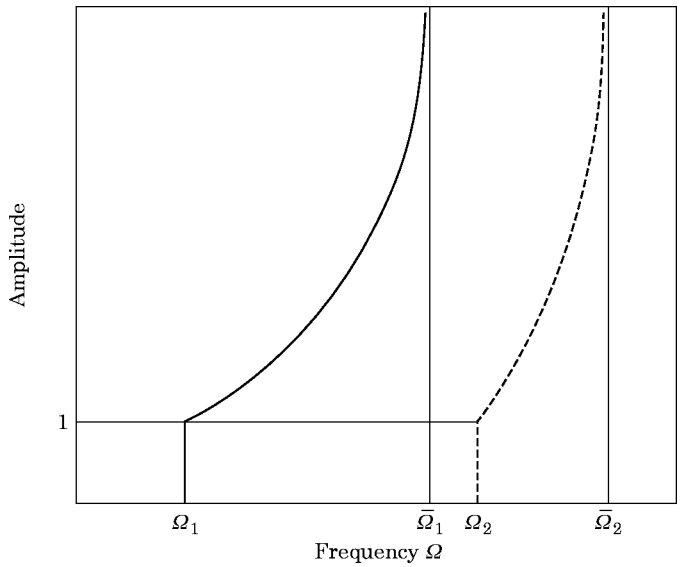

Figure 8. Schematic backbone curves for two-mode structure with a piecewise linear spring. ——, 1st backbone; - - - - - -, 2nd backbone.

one point to a piecewise linear spring of zero stiffness for normalized displacement z up to 1 and of stiffness k for larger displacement. Then for a deflection of less than 1 the structure behaves linearly and the backbone curves are vertical lines at Ω_1 and Ω_2 on the frequency spectrum. With increasing deflection the spring is engaged and the backbone curves bend to the right, this being indicative of a stiffened structure. As the displacement becomes very large relative to 1, the structure displays a nearly linear response, because at this stage the influence of the gap is insignificant. Consequently the backbone curves for the first and second modes would approach asymptotically by $\bar{\Omega}_1$ and $\bar{\Omega}_2$, respectively, which are the normalized linear frequencies for the combined system of the structure and a spring of stiffness k. Figure 8 illustrates this behaviour.

For a spring deflection larger than 1, the backbone curves contain higher harmonics of $i\theta$, where i takes on integer values starting from 2. For piecewise linear systems with symmetric force–displacement relationships higher odd harmonics would be present, and for unsymmetric systems both higher even and odd harmonics would occur. Consider that the two-mode structure is vibrating in its first mode near its first natural frequency Ω_1 with the spring deflection greater than 1; then the nth harmonic would be oscillating near the second frequency Ω_2. For mode interaction to take place the vibrating shape of the system would have to shift to the second mode, meaning that the structure would bifurcate and branch out onto an alternative equilibrium path. It seems that for this to be possible the backbone curve for the first natural frequency must intersect the second backbone curve plotted with its frequency value divided by n, as this intersection is effectively a bifurcation point.

Whether or not the two curves intersect depends on the value of the stiffness k and also on the relative participation of the spring in the two modes. As seen in Figure 8, the spring shifts both backbone curves, and the extent of the movement is a function of the aforesaid factors. If the spring is located at a node where the displacement is principally accounted for by the first mode and negligibly by the second mode, then the first backbone curve is hardened substantially more than the second. Furthermore if k is sufficiently high then the first backbone curve may be flattened enough to cut across the second curve as pictured

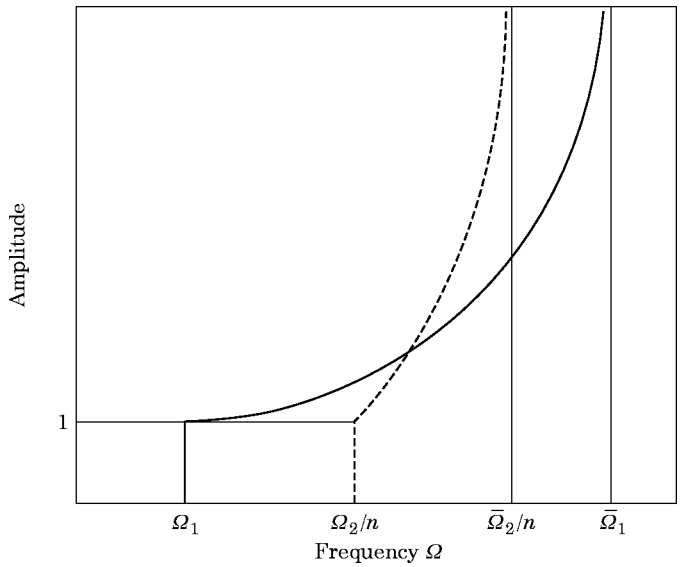

Figure 9. Schematic intersection of backbone curves for a two-mode structure with a piecewise linear spring. ——, 1st backbone; - - - - - - , 2nd backbone (Ω divided by n).

in Figure 9. It is seen that the frequency $\bar{\Omega}_1$ is higher than $\bar{\Omega}_2/n$ and that the backbone curves intersect to yield a bifurcation point where internal resonance can take place. The L beam can be used to demonstrate this phenomenon. With 10 modes, k_2 values of 0·01576 and 0·01802, the backbone curves have been computed with one harmonic to check for intersections, and results are plotted in Figure 10. The elbow undergoes high displacement in mode 1 and is near an inflection point in mode 2, and so the first backbone curve is moved considerably to the right, whereas the second curve basically remains at

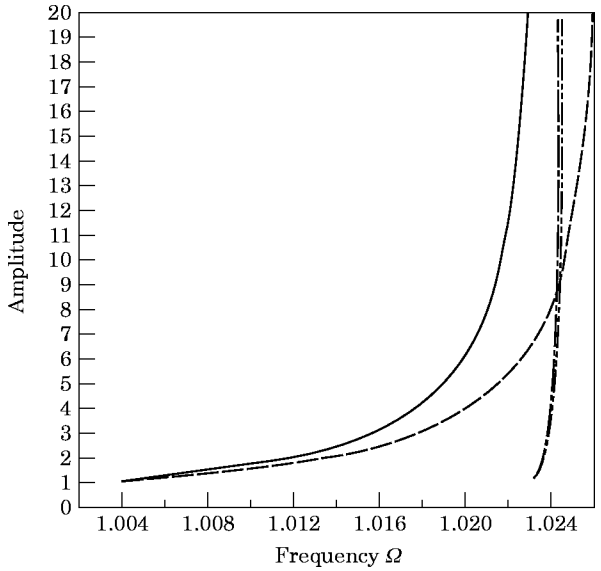

Figure 10. Intersection of backbone curves for L beam for different spring stiffness k_2 ($NH = 1$). —— 1st backbone, – · – · – 2nd backbone (Ω divided by 3) for $k_2 = 0{\cdot}01576$; - - - - - - 1st backbone, – · · – · · – 2nd backbone (Ω divided by 3) for $k_2 = 0{\cdot}01802$.

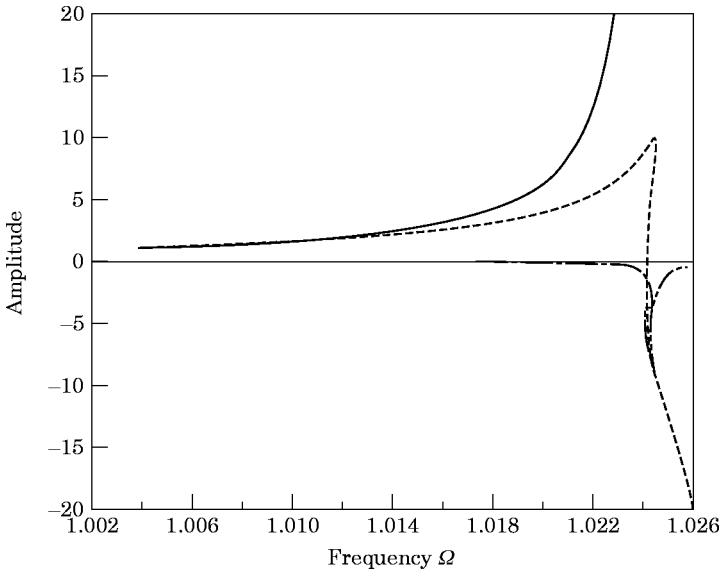

Figure 11. Amplitudes z_1, z_3 for L beam with different spring stiffness k_2 ($NH = 2$) —— z_1 for $k_2 = 0{\cdot}01576$; - - - - - - z_1, – · · – · · – z_3 for $k_2 = 0{\cdot}01802$.

the same location. The amount of stiffening induced by k_2 of 0·01576 is not sufficient to push $\bar{\Omega}_1$ beyond $\bar{\Omega}_2/n$; however, this is achieved for k_2 of 0·01802. For the latter case the two curves meet at the frequency of about 1·026 and displacement z_1 of 9·7, the bifurcation point. The actual response computed with two harmonics necessary for picking up mode interactions behaviour confirmed the prediction and the result is shown in Figure 11, where z_3 for $k_2 = 0{\cdot}01576$ is almost 0 and is not shown.

5. CONCLUSIONS

The versatility of the IHB method has been demonstrated once again in this application to analyze the internal resonance behaviour of a L beam. The elaborate nature of mode interaction is seen through the response of the individual harmonics, which show how the amplitude of one mode is diminished in favour of another as a result of the presence of higher harmonic components. It has been shown that a rarely seen high number of modes, five, participate in multiple internal resonances. This characteristic is preconditioned by the existence of frequency ratios close to integer values, and by the sufficiently high stiffness and appropriate location of the limit stop so as to cause the backbone curves of the frequencies concerned to intersect at a point. On the later aspect it is further revealed that if the stiffness of the limit stop is too soft no internal resonance could occur, and hence there is a critical stiffness above which mode interactions could take place.

It is also evident that the stop's stiffness may be selected to affect resonance between a linear natural frequency and the desired number of higher frequencies. Conversely, internal resonance may be avoided or eliminated by softening or changing the placement of the non-linear elements present. This approach can be a significant addition to the arsenal of non-linear vibration control techniques and should continued to be developed. A logical next step is to expound the interaction between the non-linear stiffness characteristic and the internal resonance under the action of periodic loading, a topic which is covered in part II of this paper [5].

REFERENCES

1. C. W. Wong, W. S. Zhang and S. L. Lau 1991 *Journal of Sound and Vibration* **149,** 91–105. Periodic forced vibration of unsymmetrical piecewise-linear systems by incremental harmonic balance method.
2. S. L. Lau and W. S. Zhang 1992 *Journal of Applied Mechanics* **59,** 153–160. Nonlinear vibration of piecewise-linear systems by incremental harmonic balance method.
3. K. Murakami and H. Sato 1990 *Journal of Vibration and Acoustics* **112,** 508–514. Vibration characteristics of a beam with support accompanying clearance.
4. S. L. Lau, Y. K. Cheung and S. Y. Wu 1984 *Journal of Applied Mechanics* **51,** 837–843. Nonlinear vibration of thin elastic plates.
5. D. Pun, S. L. Lau and Y. B. Liu 1996 *Journal of Sound and Vibration* **193,** 1037–1047. Internal resonance of an L-shaped beam with a limit step: part II, forced vibration.